

Jacqueline Caplan-Auerbach · Stephen R. McNutt

New insights into the 1999 eruption of Shishaldin volcano, Alaska, based on acoustic data

Received: 5 December 2001 / Accepted: 22 November 2002 / Published online: 4 February 2003
© Springer-Verlag 2003

Abstract Data collected by a pressure sensor provide new insights into the 1999 eruption of Shishaldin volcano, Unimak Island, Alaska. On 19 April 1999, after 3 months of unrest and an extended period of low-level Strombolian activity, Shishaldin experienced a Subplinian eruption (ash plume to >16 km), followed by several episodes of strong Strombolian explosions. Acoustic data from the pressure sensor allow us to investigate the details of an eruption which was instrumentally well recorded, but with few visual observations. In the 12 h prior to the Subplinian phase, the pressure sensor detected a series of small, repeated pulses with a constant spectral peak at 2–3 Hz. The amplitude and occurrence rate of the pulses both grew such that the signal became a nearly continuous hum just before the Subplinian eruption. This humming signal may represent gas release from rising magma. The main Subplinian phase was heralded by (1) the abrupt end of the humming signal, (2) several pulses of low-frequency sound interpreted as ash bursts, and (3) a dramatic increase in seismic tremor amplitude. The change in acoustic signature at this time allows us to precisely time the start of the Subplinian eruption, previously approximated as the time of strongest tremor increase. The 50-min Subplinian phase actually contained several bursts of signal, each of which may represent a discrete volume of magma passing through the system. Following the Subplinian event, the pressure sensor recorded four discrete episodes of Strombolian gas explosions on 19–20 April and another on 22–23 April. Four of the five episodes were accompanied by strong seismic tremor; the fifth has not been previously recognized and was not associated with anomalous tremor

amplitudes. In time series these events are similar to explosions recorded at other volcanoes but in general they are much larger, with maximum amplitudes of >65 Pa at 6.5 km from the vent, and they have low (0.7–1.5 Hz) peak frequencies. These large explosions occurred at rates of 3–20 per minute for 1–5 h in each episode. The explosions were accompanied by a small (<5 km above sea level) ash plume and only minor amounts of ejecta were produced. Thus, the explosion activity was dominated by gas release.

Introduction

Shishaldin volcano is one of six volcanoes comprising Unimak Island, the easternmost island in the Aleutian arc. Although the exact number of eruptions is uncertain, Shishaldin has erupted at least 29 times since 1755, placing it among the most active volcanoes in Alaska (Miller et al. 1998). The most recent eruption took place in April 1999, and was well documented by a seismic network, remote-sensing satellites, a pressure sensor and field visits.

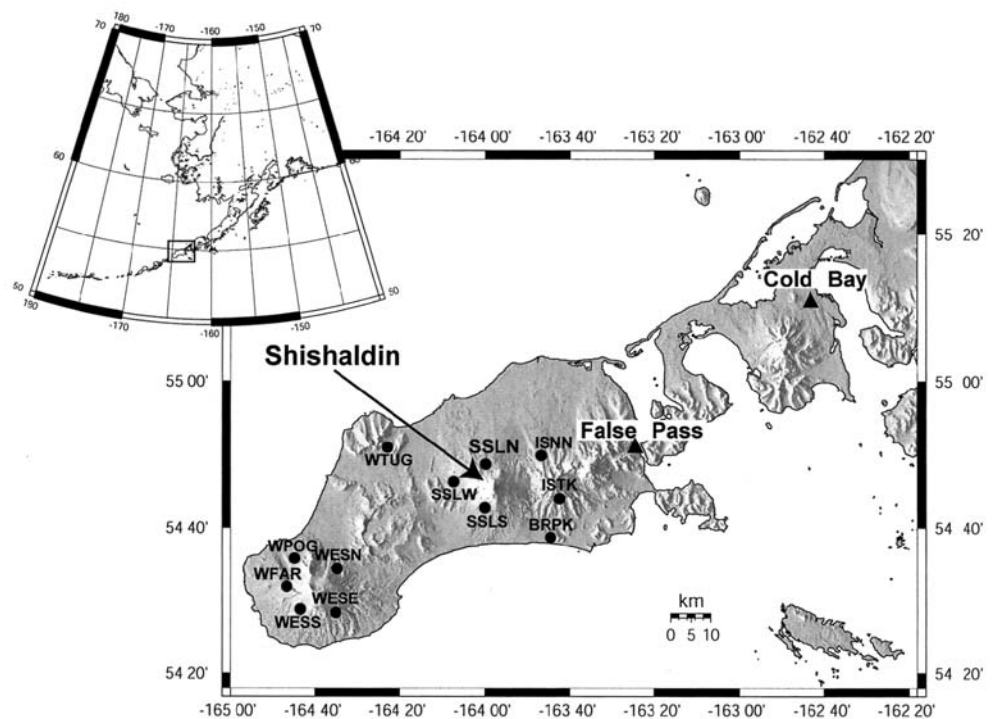
There are two populated regions near Shishaldin (Fig. 1). The nearest community, False Pass, is only 32 km away but its view of Shishaldin is blocked by Roundtop volcano. As a result, most visual observations of the 1999 eruption came either from the town of Cold Bay, 90 km from the volcano (Fig. 1), or from pilot reports (Nye et al. 2002). Observations of the eruption were further limited by poor weather. Thus, understanding the dynamics of Shishaldin's eruptive behavior relies on analysis of telemetered seismic, acoustic and satellite data.

Studies of the 1999 eruption have focused on its seismicity (Thompson et al. 2002; Moran et al. 2002), geology (Stelling et al. 2002), appearance in satellite data (Dehn et al. 2002) and eruption response (Nye et al. 2002). This paper presents data from the eruption as recorded by a pressure sensor positioned on the volcano's north flank. We begin with an overview of the data and a

Editorial responsibility: A. Woods

J. Caplan-Auerbach (✉) · S. R. McNutt
Alaska Volcano Observatory, Geophysical Institute,
University of Alaska Fairbanks,
903 Koyukuk Dr., P.O. Box 757320, Fairbanks,
Alaska, AK 99775-7320 USA
e-mail: jackie@giseis.alaska.edu
Tel.: +1-907-4746014
Fax: +1-907-4745618

Fig. 1 Map of Shishaldin volcano and Unimak Island, the easternmost island in the Aleutian arc. The seismic stations surrounding Shishaldin and Westdahl volcanoes are marked with closed circles. Closed triangles represent the two communities nearest Shishaldin, False Pass and Cold Bay. The pressure sensor is co-located with station SSLN on Shishaldin's north flank. The inset map shows the location of Unimak Island within the Aleutian chain



summary of the eruption sequence as detected by a variety of monitoring tools. Next we present several types of acoustic signals recorded on the pressure sensor, and interpret them in the context of the overall eruption. We then use the acoustic data to develop a new detailed chronology of the 1999 Shishaldin eruption, and to evaluate the transition between Strombolian and Subplinian eruptive activity. In short, data from the pressure sensor offer a more detailed view of the 1999 eruption of Shishaldin, and provide a window into eruptive processes which could not be determined by other volcanic monitoring tools.

Data collection

In July 1997, a network of six short-period seismometers and one pressure transducer was deployed on Shishaldin volcano, between 5 and 19 km from Shishaldin's central vent (Fig. 1), by the Alaska Volcano Observatory (AVO). An additional six-station network was installed on Westdahl volcano, west of Shishaldin (Fig. 1) in 1998. Five of the six seismometers on Shishaldin are short period ($T = 1$ s), vertical component geophones. The station at SSLS is a three-component station with 0.5-s period. The instrument used for detection of acoustic signals is a Setra 239 differential pressure sensor co-located with station SSLN on the volcano's north flank (Fig. 1). The pressure sensor has a flat response for frequencies <100 Hz and sensitivity of 0.2 mV/Pa. It is mounted on the eastern side of the instrument hut with a downward-pointing intake tube. This is usually the downwind side of the hut and, from this vantage point,

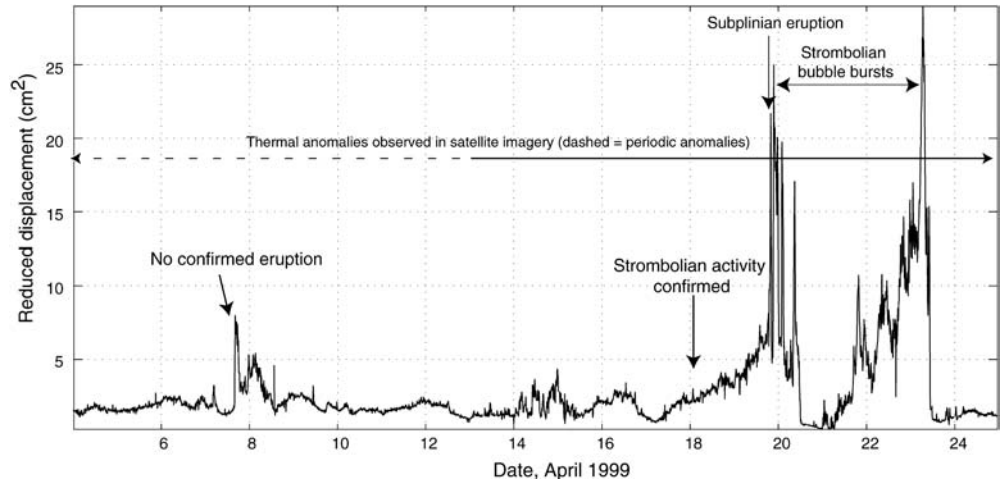
the instrument has a line of sight to the volcano's summit. Although the relative insensitivity of this instrument is unfortunate (other pressure transducers used for volcanic infrasound have sensitivities of ~ 10 –500 mV/Pa), it means that volcanic signals detected by the pressure transducer were of significant (>5 Pa) amplitude. Data for all instruments are telemetered to AVO in Fairbanks, where they are digitized at 12 bits and sampled at 100 Hz. The seismic data are analyzed at AVO in real time using the IceWeb system (Benoit et al. 1998). Further analyses for this paper were performed on archived data using MATLAB and Datascope software.

Satellite monitoring by AVO is achieved via satellites sensitive to thermal anomalies and volcanic plumes. High-resolution data (1.1 by 1.1 km pixel size at zenith) from an advanced very high resolution radiometer (AVHRR) sensor are collected approximately 10–12 times per day. Geosynchronous operational environmental satellite (GOES) data are acquired approximately every 15 min. The combination of seismic and satellite data allow AVO to monitor the volcano's activity even when local visual observations are not possible.

Eruption onset and chronology

Eruption chronology is best documented by the seismic and pressure data, both of which provide continuous signals. The seismic signal consists of volcanic tremor and earthquakes, whereas the pressure data consist of three types of signal described below. Tremor amplitude is represented by the reduced displacement (D_r), a parameter which corrects for geometric spreading with

Fig. 2 Chronology of tremor amplitude for April 1999. Three main phases of tremor increase occurred on 7–8, 18–20, and 21–23 April. Also noted are times when eruptive activity or thermal anomalies were observed



distance to the seismometer. D_r has been shown to correlate positively with volcano explosivity index (VEI) and ash column height (McNutt 1994). Seismic tremor was first observed on Shishaldin in February 1999, coincident with observations of a puffing steam plume at Shishaldin's summit (Nye et al. 2002). In hindsight, faint tremor was identified as early as January 1999, but at the time was not distinguished from wind noise. A thermal anomaly first seen at Shishaldin on 9 February (all dates and times in UTC) persisted throughout the period of unrest (Nye et al. 2002). Throughout the months of March and April 1999, D_r steadily increased until 7 April when it reached levels commonly associated with $VEI=2$ eruptive activity ($5\text{--}7\text{ cm}^2$; Fig. 2). Unfortunately, poor weather precluded visual or satellite observations of the volcano at that time, so there was no confirmation that an eruption accompanied this heightened activity. Tremor amplitude returned to background levels ($1\text{--}2\text{ cm}^2$) by 8 April. An increase in D_r was once again observed on 17 April and, on 18 April, AVO staff equipped with a forward looking infrared radiometer (FLIR) observed Strombolian eruptive activity on an overflight of Shishaldin (Nye et al. 2002; Fig. 2).

Tremor amplitudes continued to rise throughout 19 April, with rapid increase beginning at 19:30 UTC (Fig. 2). In the absence of visual observations to confirm the timing of events, this increase in tremor amplitude has been designated the initiation of the Subplinian eruption (Thompson et al. 2002). Satellite imagery traced the development of the resulting plume from 19:45–22:30 UTC as it rose to $>16\text{ km}$ (Schneider et al. 1999). D_r values decreased dramatically from 23 to 1 cm^2 after the Subplinian eruption, but increased again three times on 19–20 April, then once more on 22 April, eventually surpassing the D_r values recorded prior to the 19 April eruption. The strongest tremor recorded at Shishaldin occurred between 5:00 and 10:00 UTC on 23 April ($D_r=43\text{ cm}^2$), after which time D_r values subsided dramatically. Satellite data also indicate the strongest thermal anomaly on 23 April – a 31-pixel anomaly recorded by the AVHRR satellite (Dehn et al. 2002). With

corrections for zenith angle and topography, this translates to an area of $\sim 25\text{ km}^2$, and confirms that hot material was ejected at least 3–4 km from the summit. GOES imagery at this time shows a small, ash-poor eruption plume (Schneider et al. 1999; Nye et al. 2002). Tremor levels remained low ($<2\text{ cm}^2$) after 23 April, although several small ash and steam plumes were observed in late April and May. Although Strombolian activity was observed a number of times during the month of April, the Subplinian eruption of 19 April is believed to be responsible for the vast majority of erupted material and only a single deposit could be discerned in the field (Stelling et al. 2002).

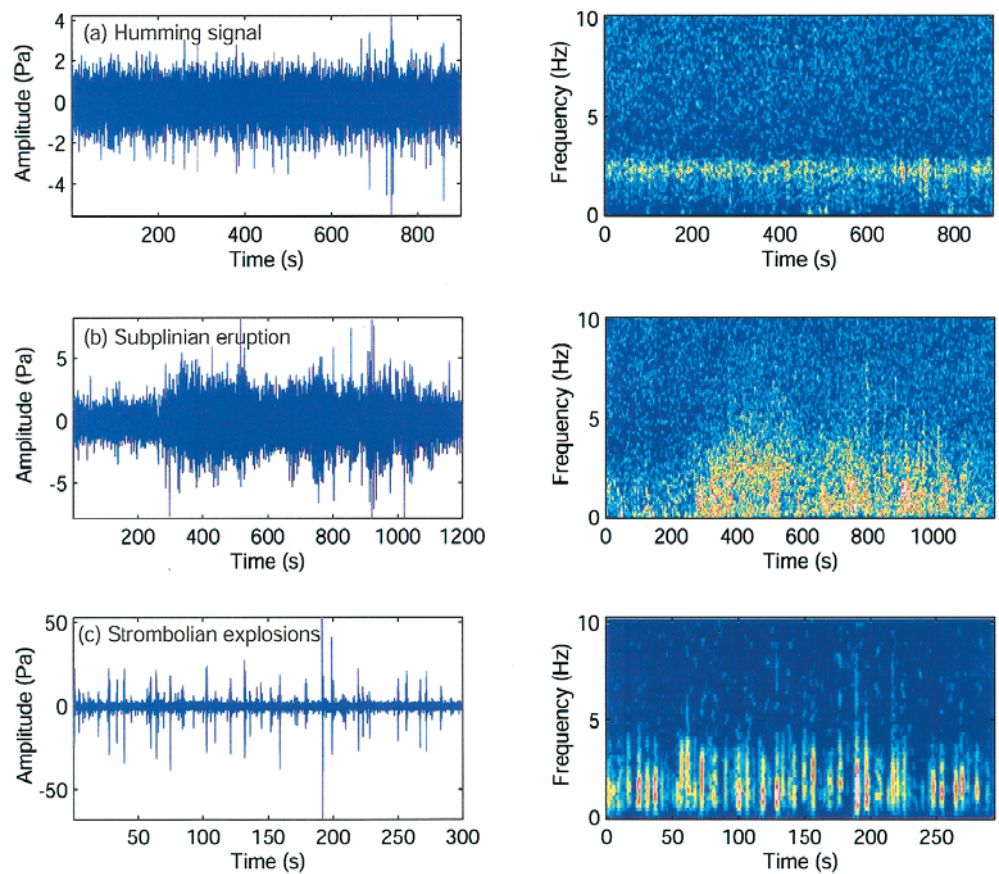
The combination of seismic and satellite data provide significant insight into an eruption which was largely hidden from visual observations. However, it is not certain what kind of physical processes led to and followed the main Subplinian eruption. Furthermore, because seismic energy passes through the earth, it offers a filtered view of source processes. To better address these issues, we examine data collected by the pressure sensor, which provides a more direct view of source processes.

Acoustic data

There are three different signals detected by the pressure sensor in 1999 which were associated with eruptive activity. These are (1) a steady, 2–3 Hz hum; (2) a diffuse broadband signal at the time of the Subplinian eruption; and (3) discrete, repeating pulses lasting 1–3 s (Fig. 3). We investigate each of these signals in turn to determine their relationship to the volcano and what they indicate about the eruption. We also use these data to determine first-order conduit processes active during the eruption, although a full quantitative analysis of these processes is the subject of another paper.

Before deciding that a signal detected by the pressure sensor is of volcanic origin, we must consider the contribution of other sources to the pressure sensor

Fig. 3a–c Time series and spectrograms for the three different acoustic signals detected by the pressure sensor during the 1999 Shishaldin eruption. **a** 2–3 Hz humming signal, 19 April 1999. Time series begins at 19:00 UTC. **b** Broadband signal associated with the main Subplinian eruption, 19 April 1999. Time series begins at 19:35 UTC. **c** Discrete events interpreted to be gas explosions, 23 April 1999. Time series begins at 7:30 UTC. For all spectrograms, *blue* represents weak signal, *yellow* intermediate, and *red* strong signals. Note that the time series have different horizontal and vertical scales, whereas spectrograms have the same vertical (frequency) scales



record. The pressure transducer was deployed in such a way as to diminish wind noise, with a hose to the pressure port oriented toward the ground and thus away from the wind. Even so, wind cannot be completely ruled out as a source of acoustic signals. Wind speeds are typically high in the Aleutians, and background D_r has been shown to correlate with wind strength measured at Cold Bay, 90 km from Shishaldin (Nye et al. 2002). Cold Bay is the nearest meteorological station, and we assume conditions there are similar to those at Shishaldin. The appearance of wind noise in the pressure record is therefore not well known. Cold Bay wind data are collected hourly, so short-period gusts are not reflected in the record, and wind azimuth is recorded only once per day. Acoustic signal strength was intermittently high during strong winds (>15 knot) on 19 and 21 April, but other days with high winds (e.g., the afternoon of 24 April when wind speed in Cold Bay exceeded 20 knot) show no anomalous pressure signal. Most of the pressure signals discussed in this study occurred only during times of known eruptive activity and are believed to be directly associated with the volcano.

As a further check of a pressure signal's volcanic origin, we attempted to correlate signals detected by the pressure sensor with signals found in the seismic record. This process was complicated by the fact that during much of the 1999 eruption, the seismic traces were saturated (clipped), often masking individual signals. Although seismic tremor amplitude generally increased

during the 2–3 Hz humming signal, no notable peak at that frequency band is visible in the seismic data. Tremor frequency was typically a broad peak between 0.5 and 3.5 Hz. The broadband signal which we attribute to the Subplinian eruption is visible in both the acoustic and seismic records. Furthermore, an increase in tremor amplitude was observed whenever explosion signals were seen in the acoustic data. Although saturation of the seismic records was problematic, air waves correlating with explosive signals were visible for some events on one of the farther seismic stations, ISNN (Fig. 4). Because ISNN is located ~ 8 km farther from the vent than is station SSLN, the seismic data are offset by the approximate travel time for an acoustic signal with velocity of ~ 320 m/s. We hoped to identify the preceding ground waves associated with each air wave, but such events were masked by strong tremor.

Humming signal

We begin by discussing the signal which most directly preceded the Subplinian eruption. At $\sim 7:00$ UTC on 19 April, the pressure sensor recorded a low-amplitude, nearly continuous “humming” signal (Fig. 3a). This signal is strongly band-limited between 2 and 3 Hz. Between 7:00 and 19:30 UTC, signal amplitude increased by a factor of 2, achieving maximum amplitudes of ~ 5 Pa at

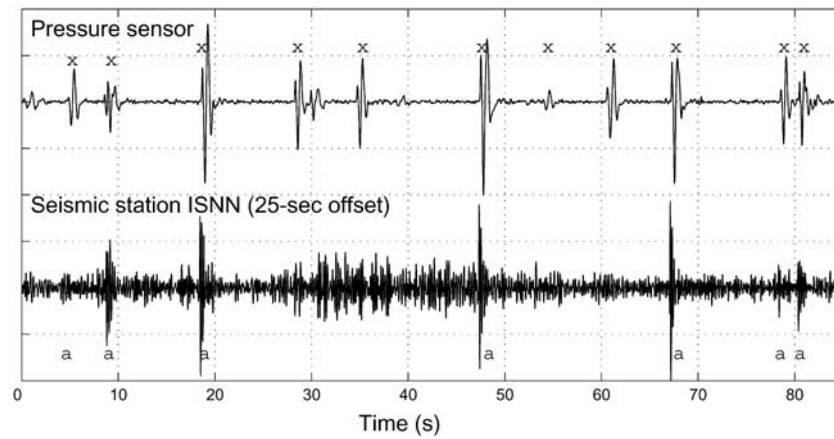
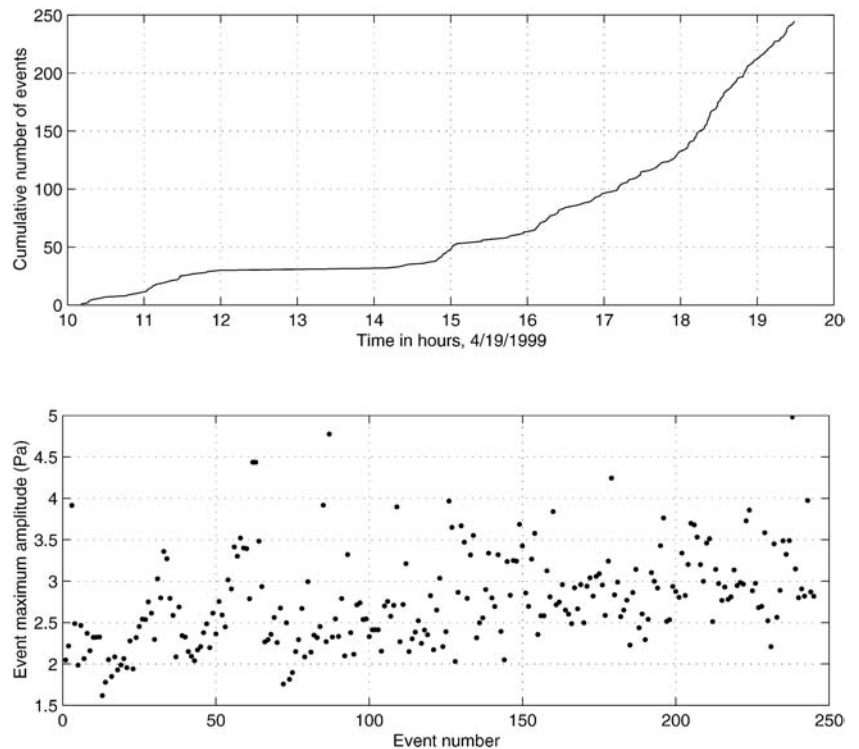


Fig. 4 Explosions detected by the pressure sensor (SSLN) and airwaves recorded at seismic station ISNN. Explosions are marked with an *x* and airwaves are marked with an *a*. The pressure sensor trace begins at 10:03:10 UTC. The trace for station ISNN begins at 10:03:35, offset by 25 s (the travel time difference for air waves arriving at the two stations) relative to the upper trace, so that the

explosion events are aligned. The seismic trace has been highpass-filtered above 5 Hz to diminish signal from tremor and amplify the appearance of the air waves. Ground waves resulting from the explosions are masked by tremor and cannot be identified in the seismic time series

Fig. 5 Number and amplitude of “hum” events, 19 April for the time period between 10:00 and 19:35 UTC. Both the number per unit time and amplitude of these events increased with time. The signal abruptly ended 4 min before the Subplinian eruption at 19:39 UTC. The events shown here are a subset of hum events which were selected for their similarity; all events shown here were similar (coherence>0.90) to a reference event which occurred shortly before the Subplinian phase



6.5 km from the vent in the half hour preceding the eruption (Fig. 5). The strong spectral peak at 2–3 Hz never changed throughout this time period (Fig. 6).

Closer examination of the hum shows that it is composed of a series of explosion-like pulses (Fig. 7) several seconds apart. Unlike other discrete signals detected on the Shishaldin pressure sensor, most of these events cycle through several wavelengths; other explosion signals attenuate after a single wavelength. This suggests either a source process which resonates for several cycles

or energy passage through a medium with relatively poor attenuation.

To determine whether the signal was indeed repetitive, we performed cross-correlation analysis and extracted all events between 10:00 and 19:30 UTC which were similar (coherence >0.9) to a reference event. We chose 10:00 as the start time for the cross-correlation analysis because of the relatively weak signal strength prior to that time. A pulse which occurred just prior to the end of the humming episode was selected as the reference event because it had

Fig. 6 Power spectra for the 2–3 Hz hum. Spectra are calculated for 30-min windows preceding the Subplinian eruption at 19:39 UTC on 19 April. The amplitude of the humming signal increases over the 4.5 h shown, but the peak frequency of 2–3 Hz remains constant

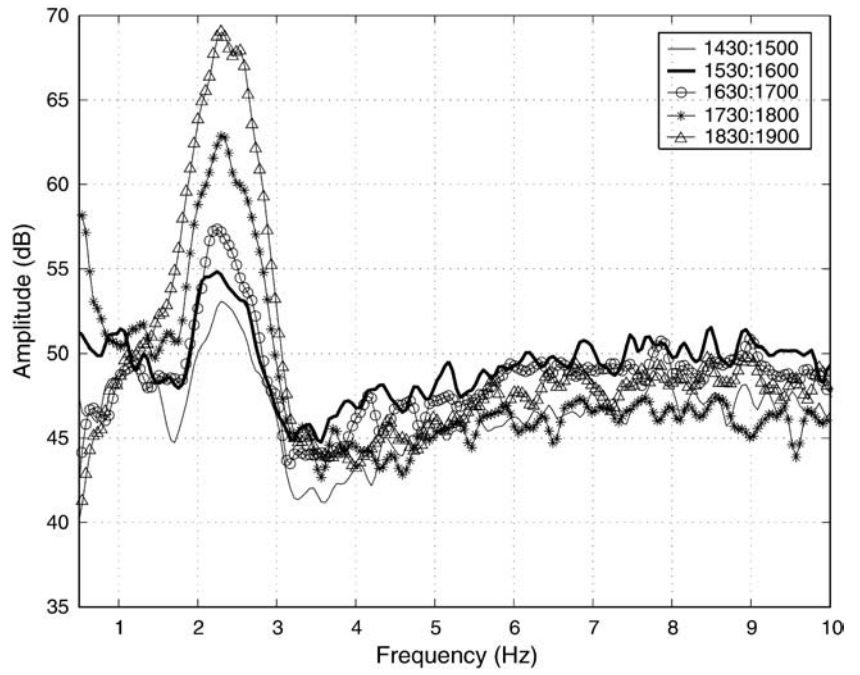
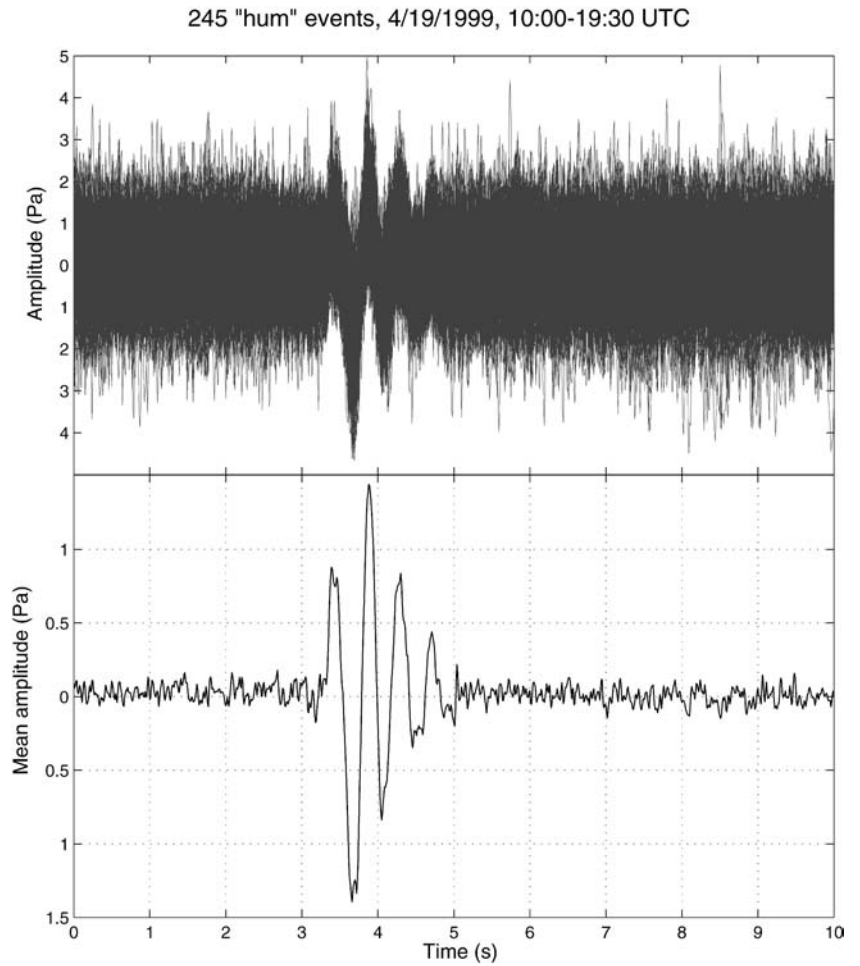


Fig. 7 Plots showing the 245 overlaid time series of normalized 2–3 Hz signal in acoustic data, and the stack of these 245 pulses. The signal retained its waveform and power spectrum throughout the ~12 h period during which it was observed



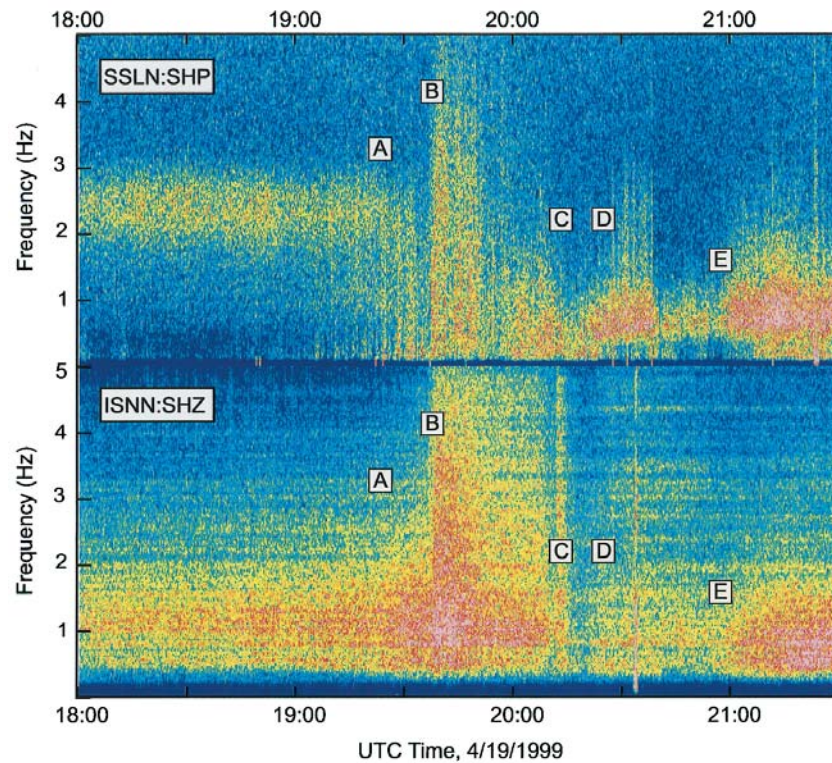


Fig. 8 Spectrograms for the 3.5 h surrounding the Subplinian eruption of 19 April 1999. The *top panel* shows data from the pressure sensor. The *bottom panel* is seismic station ISNN for the same time period (station SSLN, co-located with the pressure sensor, clipped during this time period). Spectra are calculated for a 1,024-point signal (10.24 s), with 80% overlap. The data have been highpass-filtered at 0.1 Hz to reduce microseism noise. Time A (19:25) marks the end of the 2–3 Hz hum and the beginning of low-

frequency signals believed to be small ash bursts. Time B (19:39) marks the broadband signal interpreted to be the onset of the main Subplinian eruption. Time C (19:55) represents the tapering of the second Subplinian pulse. Time D (20:28) denotes the beginning of discrete signals interpreted to be Strombolian gas explosions. A second burst of explosions begins at time E. Note the increase in tremor amplitude coincident with the end of the 2–3 Hz humming signal just after time A

a strong signal-to-noise ratio, and the start and end times were easy to define. In all, 245 events meeting these criteria were found, and we observe that their amplitude and occurrence rates increase with time (Fig. 5). In the half hour prior to the end of the humming signal, the pulses occur so frequently that they become nearly continuous. We note that there may be other pulses contained within the continuous record which do not exceed the coherence criteria. Furthermore, because the reference event occurred near the end of the episode, the increase in event occurrence rate may simply reflect a temporal change in event appearance toward that of the reference event. Such a trend would suggest a source slowly changing with time. Humming pulses which occurred near the beginning of the episode were too small to extract from the data without the cross-correlation method and therefore could not be used as effective reference events. However, we were able to repeat the analysis for a reference event which occurred midway through the sequence, and noted the same general increase of amplitude and occurrence rate. Thus, the analysis appears to be robust.

Subplinian phase

On 19 April at 19:25 UTC, after more than 13 h of continuous amplitude increase, the 2–3 Hz hum began to decline (Fig. 8, time A). At this time, several low frequency (~1–2 Hz) bursts appeared in the pressure record. This time precisely coincides with a dramatic increase in tremor amplitude (Fig. 8). These data together suggest a change in physical process. By 19:35 UTC, the 2–3 Hz hum has disappeared, and tremor amplitude continues to build. At 19:39 UTC (Figs. 3b and 8, time B), the pressure record reveals a strong, 14-min signal unlike any of the signals previously detected by the instrument. This signal is composed of a relatively broadband (1–10 Hz) background over which is superimposed a series of strong, low-frequency pulses at 1–2 min intervals. The low-frequency (<1.5 Hz) portion of this signal continues until ~20:30 UTC (Fig. 8, time C), at which point the pressure record shows a shift to slightly higher (0.5–3 Hz) frequencies. Seismic records show a similar pattern – a strong broadband signal at 19:39 UTC, tapering to lower frequencies and decreasing dramatically by 20:30 UTC. Because satellite records indicate that this time period coincides with the main ash-producing episode of the

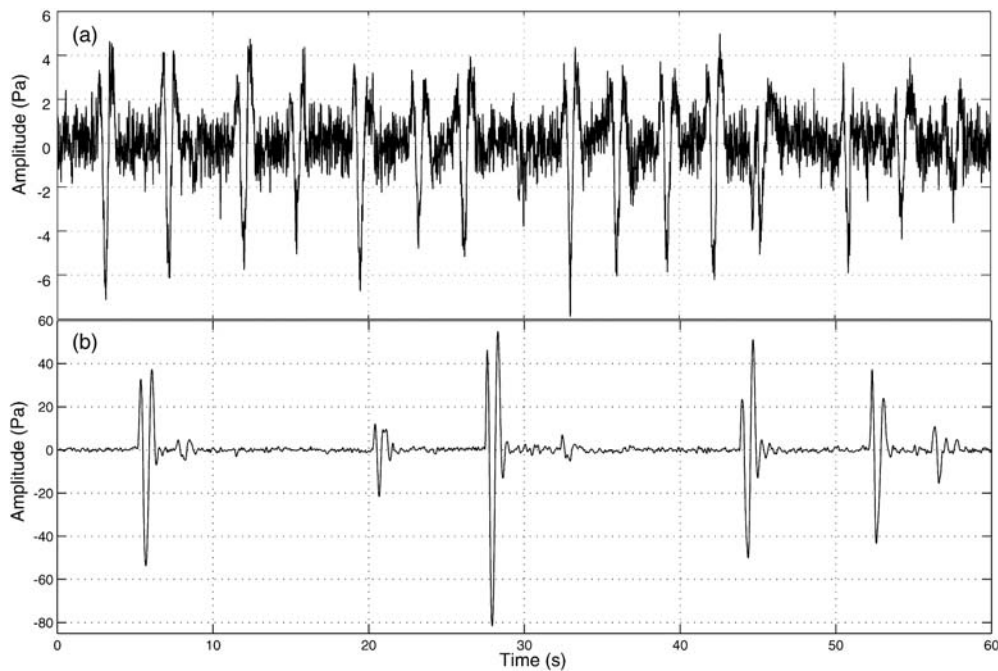


Fig. 9. **a** One-minute time series for explosions recorded on 19 April 1999, beginning at 23:06:10 UTC. These signals have a low-frequency (0.7–0.8 Hz) onset. No coda is visible over background noise. **b** One-minute time series for explosions recorded on 23 April 1999, beginning at 09:59:15 UTC. Most signals begin with a low-frequency (1.3 Hz) pulse, followed by a higher-frequency (2–4 Hz)

coda. Vergnolle and Brandeis (1994) suggest that the low-frequency signals represent gas bubbles vibrating at the magma–air interface and that the high frequencies result from the bubble popping. Although more explosions are visible for this particular 19 April segment, in general all eruptive episodes had similar event occurrence rates

Table 1 Explosion data, Shishaldin volcano 1999 eruption

	Episode start time (UTC)	Episode duration	Estimated number of events ^a	Event rate (events per minute)	Event peak frequency (Hz)	Event mean amplitude (Pa)	Event maximum amplitude (Pa)
Episode 1	19 April, 20:25	15 min	110	6.9	0.7	4	10
Episode 2	19 April, 21:00	2.75 h	1,090	6.6	0.7	4	8
Episode 3	20 April, 01:33	1 h	310	1.7	1.1	2	10
Episode 4	20 April, 07:55	2 h	530	4.6	1.3	1.5	5
Episode 5	22 April, 22:30	1.5 h	590	3.3	1.3	1.5	8
	23 April, 00:00	3 h ^b	850	4.7	1.5	2	7
	23 April, 05:00	5.25 h	2,200	7.0	1.3	10	66

^a Events selected using short-term average/long-term average ratio ^b Few explosions visible at 03:00–05:00 on 23 April; pressure record appears noisy at 0.5–3 Hz

eruption, we conclude that this ~50-min period represents the Subplinian phase of the eruption.

Explosions

At 20:30 UTC, the broadband signal ceases and is replaced by a series of discrete, impulsive pulses which we interpret to be explosions caused by bursting gas bubbles in the magma (Fig. 8, times D and E). Waveforms for these events generally exhibit an initial low-frequency oscillation often followed by a low-amplitude, higher-frequency coda (Fig. 9). Explosion strength varies, but the largest events on 19 April have amplitudes of ~10 Pa at a distance of 6.5 km from the vent (Table 1). The

explosions occur at irregularly spaced intervals of 3–20 s. Each explosion has a 1–3 s duration, so some events with complicated waveforms may result from two or more explosions closely spaced in time (<1 s), or may indicate a more complex source process. We see no apparent relationship between recurrence interval and event amplitude. These events are low frequency, with spectral peaks between 0.7 and 0.8 Hz (Table 1).

The explosion signals continue until 23:45 UTC on 19 April. Similar explosions were recorded twice more in this phase of the Shishaldin eruption – at 1:30–2:30 UTC and at 7:55–9:30 UTC on 20 April (Table 1). Each of these time periods corresponds to an increase in tremor amplitude and decrease in tremor mean frequency, as reported by Thompson et al. (2002). Thompson et al.

(2002) suggest that the frequency decrease indicates a drop in the velocity of compressional waves in the conduit, potentially related to an increase in magma gas content (increasing the gas content changes the bulk compressibility, thereby lowering the acoustic velocity in the magma). The presence of explosions in the acoustic data recorded during these time periods supports this view.

Similar explosions were again recorded on the pressure sensor on 22 and 23 April, at a time when D_r values were escalating (Table 1). In fact, D_r values calculated on 23 April were the strongest ever recorded by AVO, exceeding 43 cm^2 (Thompson et al. 2002). The largest thermal anomaly recorded during the eruption was observed in AVHRR data at this time, indicating that hot material covered $\sim 25 \text{ km}^2$ of Shishaldin's flanks (Dehn et al. 2002). Explosion signals are common in the pressure record after 22:30 UTC on 22 April, and continue until 10:15 UTC on 23 April (Table 1). Between 03:00 and 05:00 UTC on 23 April, few explosions are observed in the pressure record, perhaps owing to a strong, 0.5–3 Hz signal which is indistinguishable from noise. The explosions recorded on 22–23 April are larger than explosions recorded on the 19th or 20th, with maximum amplitudes $>60 \text{ Pa}$ on 23 April, although they have higher peak frequencies ($\sim 1\text{--}1.5 \text{ Hz}$; Table 1). Satellite data confirm that a small ash plume was generated at this time, but no distinct fall deposit was identified (Stelling et al. 2002). It is probable that the explosions of 22–23 April did not generate much ash but ejected small bombs and lava fragments over much of the volcano's flanks. This widespread hot debris from both the observed ash plume and Strombolian explosion ejecta accounts for the broad thermal anomaly observed at that time (Dehn et al. 2002).

Discussion

The 1999 Shishaldin eruption is important for volcanology in part because three types of eruptive activity occurred – Strombolian eruptions were observed on 18, 21 and 22 April, a Subplinian eruption took place on 19 April, and strong Strombolian explosions caused by magma bubble bursts were acoustically recorded on 19–20 and 22–23 April (Fig. 2). It is important to note that while all of the Strombolian phases of the eruption were composed of discrete gas and magma bursts, the activity on April 18 was significantly weaker and was not detected by the pressure sensor. By contrast, the activity following the Subplinian phase consisted of much more vigorous explosions, each of which generated a strong acoustic signature. Other small ash plumes were observed during the period of unrest but only one, on 23 April, was timed with sufficient precision to correlate with digital records (no anomalous acoustic signal was observed at that time, perhaps owing to the low sensitivity of the pressure transducer). The fact that Shishaldin exhibited not only a change from Strombolian to Subplinian activity, but also returned to Strombolian behavior makes these transitions

particularly intriguing. It also suggests that Strombolian behavior is the norm for Shishaldin (a point also cited by Miller et al. 1998), and that something anomalous occurred to trigger the Subplinian phase. The humming signal recorded by the pressure sensor provides a small window into the processes which triggered this explosive phase.

The processes by which a basaltic volcano may exhibit Subplinian or Plinian behavior are poorly understood. When rocks from the 1999 eruption were sampled, no distinction could be made between deposits produced during the separate eruptive phases (Stelling et al. 2002). Although it is possible that not all of the phases were sampled, we infer that the magmatic chemistry did not change significantly over the course of the eruption. Instead, we believe that the different eruptive processes resulted from changes in gas content, gas exsolution processes or magma ascent rate.

Subplinian basaltic eruption mechanisms

Subplinian or Plinian basaltic eruptions have been observed on only a few volcanoes, including Masaya (Williams 1983), Tarawera (Walker et al. 1984), and most notably Etna which has experienced 24 Plinian or Subplinian eruptions in the past 13 ka (Coltelli et al. 1995). Sable et al. (2001) suggest that microlite crystallization within the Etna conduit could result in an increase in magma viscosity, thereby forming a cap rock and trapping gasses within the fluid until the resulting overpressure causes it to erupt explosively. While scoria clasts from the 1999 Shishaldin eruption are microlite rich, the relative paucity of microlites at the rims shows that these crystals probably formed in flight and not within the conduit (J. Gardner, personal communication 2002). Another concern with this model is that the destruction of cap rock may be expected to generate a significant impulsive infrasonic signal (Morrisey and Chouet 1997), yet none is evident in our data. Another possibility is that the vent at Shishaldin was blocked by debris falling back into the summit crater, which then blocked the escape of gas. However, the persistence of Strombolian activity and the strong summit thermal anomalies recorded in the days prior to 19 April (Dehn et al. 2002) makes it unlikely that material within the vent could cool sufficiently to block gas release. Coltelli et al. (1995) and Houghton et al. (2001) propose that basaltic Plinian eruptions may be caused by the rapid ascent of magma, resulting in delayed and rapid vesiculation. The possibility that magma ascent rate changed at Shishaldin, such that bubbles and magma no longer rose differentially, has also been discussed by Stelling et al. (2002). This model is further supported by the increase in tremor amplitude observed before the Subplinian event (Thompson et al. 2002).

But is this model supported by data from the pressure sensor? The dominant signal in the 10 h leading up to the Subplinian phase is the 2–3 Hz hum. The relative timing of the 2–3 Hz hum and the Subplinian eruption, combined with the gradual increase in the amplitude of each signal pulse, strongly suggests that the hum results from a volcanic process related to the impending Subplinian eruption. Furthermore, the hum was not detected at any time after the Subplinian phase, implying either that the source of the hum was destroyed in the eruption or that its source process was specific to the conditions preceding the Subplinian phase. Although wind speed in Cold Bay also increased during this time period, the end of the humming signal does not appear to correlate with a change in wind speed. We also note that while seismic tremor amplitude did increase immediately prior to the Subplinian phase, there does not appear to be any significant change in tremor frequency or amplitude during the time period in which the humming signal was detected. Furthermore, although tremor is strong between 1 and 4 Hz, there is no notable peak at 2–3 Hz in the seismic record (Fig. 8). No air phases are evident in the seismic record, but any such signals may have been too small to be detected over the strong seismic tremor present at the time.

A potential cause of the humming signal is the opening of a crack or valve near the top of the conduit, through which gas can escape. In this model, a fracture is repeatedly opened under pressure from rising gas within the conduit. This model is appealing in that it explains the similarity of the humming pulses (the same source is operative throughout the humming episode). It is also reasonable to expect that, as more gas rises through the conduit, the valve opens more frequently. The nearly continuous nature of the hum suggests that the valve was set into continuous vibration just before the Subplinian eruption. A similar phenomenon has been invoked for “chugging” events at Karymsky volcano (Johnson and Lees 2000). The geometry of such a source at Shishaldin, however, is difficult to envision, given that Strombolian eruptive activity was observed at the vent the day before, and vent materials may not have cooled sufficiently to form a coherent fracture.

A second possibility is that the pulses represent a repeated bubble source such as that proposed for the explosions which occurred after the Subplinian phase. In contrast with the later explosions, however, the 2–3 Hz pulses occur so close together that they overlap in time series, effectively becoming continuous. This requires a series of small bubbles rising simultaneously, rather than individual bubbles which fill the conduit. Furthermore, the appearance of the 2–3 Hz events in time series differs from the explosions – each humming pulse has three strong oscillations with a gradually tapering coda, whereas the strongest part of the explosion signal rapidly attenuates after a single cycle (compare Figs. 7 and 9). This implies that if these signals are due to bubbles, they

were able to oscillate at the magma–air interface for several cycles prior to bursting. Gas within these bubbles is probably less overpressured during the hum than the gas released in the later Strombolian phase of activity, suggesting that the hum represents exsolution at shallower depths. This signal may therefore represent the formation of a gas-rich foam within the conduit, with small bubbles of gas coalescing within the foam and rising more rapidly. As the foam rises, more gas is exsolved, and more bubbles leave the rising magma. The similarity in the waveforms suggests that the bubbles coalesce to a similar size before bursting. GOES images taken at 19:15 and 19:30 UTC show the formation of a small steam plume well before the Subplinian phase. We contend that this plume is the product of 12 h of continuous degassing in the humming phase.

At 19:35 UTC, the humming signal stops and the pressure sensor records a few low-frequency pulses. This change also coincides with a dramatic increase in seismic tremor amplitude (Fig. 8). We infer that at this time, the gas bubbles and magma rose at the same rate, with no differential movement of discrete bubbles. Consequently, a significant amount of activity was occurring within the conduit but little acoustic energy was transmitted into the atmosphere. The low-frequency pulses at this time may represent preliminary ash bursts before the main Subplinian phase.

In the absence of visual observations, the increase of tremor at 19:35 UTC was originally interpreted as the start of the Subplinian phase (Thompson et al. 2002). We contend that the strongest burst of the Subplinian eruption began at 19:39 UTC, when a strong broadband (1–10 Hz) signal was recorded by both the pressure sensor and the seismic network (Fig. 8, time B). Another possibility is that the main Subplinian burst took place at 19:35 UTC, but was not heard at the location of the pressure sensor. During the 1980 eruption of Mt. St. Helens, a 100-km “zone of silence” resulting from refraction of acoustic waves in the atmosphere was formed around the mountain, in which no noise from the eruption could be heard (Fairfield 1980; Dewey 1985; Johnson and Malone 1997). However, the presence of other signals from the Shishaldin eruption show that sounds generated at the summit of Shishaldin easily reached the sensor, rendering this explanation less likely. Thus, we conclude that the Subplinian eruption began at 19:39 UTC.

The Subplinian phase, as recorded by the pressure sensor, continues for 49 min (Fig. 8, time period B–D), corresponding to the time period designated as “Subplinian tremor” by Thompson et al. (2002). This time period may be further divided into a broadband (1–10 Hz) pressure signal lasting until 19:53, followed by ~10 min of relative quiescence and then a 25-min low-frequency (0.5–3 Hz) signal. Although there were no visual observations of the vent at this time, we suggest that these periods represent two consecutive bursts of magma. Satellite observations also show several pulses of activity. GOES images taken at 19:30 and 19:45 UTC show an ash-poor plume whereas those taken after 20:00 UTC

show a strong, ash-rich component. Observations of the eruption plume by local pilots also suggest that the Subplinian phase was composed of two bursts (Stelling et al. 2002). It is possible that the broadband signal corresponds to the ash-poor plume but it is more likely that the first visible plume corresponds to gas release prior to 19:39 UTC. The two bursts visible in the acoustic record are likely not distinguishable within the satellite imagery. Within each of these time periods, the acoustic signal may be further decomposed into smaller units. Again, we propose that each of these subevents represents the eruption of a small volume of magma. No other data are available to confirm whether the Subplinian phase was in fact composed of multiple bursts, but a small ash plume videotaped on an AVO overflight of Shishaldin on 23 April clearly erupts several discrete pulses of gas and ash 1–3 min apart.

During the final minutes of the Subplinian phase, ~20:25 UTC (Fig. 8, time C), the seismic record shows a decrease in tremor amplitude. Signal persists at the pressure sensor throughout this time, implying that energy is being transmitted efficiently through the air but less so into the ground. We suggest that this period represents a transition time when no new magma was moving through the conduit, but acoustic signals were still being generated in the atmosphere by a previous pulse, now erupted. The combination of data from seismic and acoustic sensors thereby offers a means by which the progress of magma may be traced as it rises through the volcano and eventually loses coupling with the ground.

Gas bubble explosions

When the second low-frequency pulse diminishes at 20:28 UTC, it is replaced by the discrete pulses which we interpret to be gas explosions (Fig. 8, time D). A short episode of Strombolian explosions begins at time D with a second, more prolonged episode initiating at time E. There is no apparent difference in the pulses generated at these times; they have identical power spectra and are similar in time series. The first explosive episode, however, is associated with weak seismic tremor (low D_r) whereas the second and third pulses correlate with high D_r values. This implies that the explosions which took place in between 20:28 and 20:40 UTC coupled poorly with the ground. This could indicate bubbles bursting at the surface of a lava volume in Shishaldin's vent, while later explosions initiated deeper within the conduit. We note that these episodes differ from the periods of explosivity discussed by Thompson et al. (2002) – the first pulse discussed in that paper is the one initiating at time E. Thus, we have identified a new phase of the eruption which was not previously known to have occurred.

The explosions recorded on 19, 20, 22 and 23 April bear strong resemblance to signals recorded at Stromboli, Etna, Karymsky, Erebus, Sakurajima and Arenal volcanoes, associated with gas explosions at the vent

(Vergniolle and Brandeis 1994, 1996; Ripepe et al. 1996; Rowe et al. 1998; Garces et al. 1999; Hagerty et al. 2000; Johnson and Lees 2000; Ripepe et al. 2001). In fact, when viewed in time series, the waveforms of some Shishaldin explosions exhibit sequences of compressions and dilatations identical to explosions recorded at Stromboli in 1991 (Vergniolle and Brandeis 1994). In both cases the time series shows a low-frequency oscillation, with a small, higher-frequency signal superimposed just after the first cycle (Fig. 9). The remarkable similarity between the two pressure records suggests that the same source process is at work on both Shishaldin and Stromboli. Vergniolle and Brandeis (1994) suggest that the signal is caused by a rising gas bubble, and that the initial low-frequency signal is caused by oscillations of the bubble rim at the magma–air interface.

Several methods have been proposed by which acoustic waveforms may be used to quantify gas flux at volcanoes. Some of these methods (Firstov and Kravchenko 1996; Johnson 2000) are based on the relationship described by Lighthill (1978), which states that pressure fluctuations are proportional to the rate of change of mass flux at the source. Thus, the second time integral of the waveform, and the use of appropriate constants should yield the amount of mass released. This method, however, assumes that the entire waveform results from changing rates of mass flux. If, in fact, the pressure trace is generated by an oscillating bubble which has not yet popped, the net gas flux is zero. Consequently, use of the integrated waveform will overestimate the amount of gas released by as much as several orders of magnitude. A precise estimate of mass flux requires detailed modeling of the bubble burst waveforms and is the subject of another work. Here, we perform a semi-quantitative comparison between the Shishaldin signals and those recorded at other volcanoes.

Comparing acoustic signals recorded at different volcanoes at different distances from the source requires that they be measured on some standard scale. Johnson (2000) recommends use of the “sound pressure level” (*SPL*), a measure of signal strength at a fixed location relative to the vent and measured in dB. *SPL* is defined by

$$SPL = 20 \log \left(\frac{\Delta P}{2 \times 10^{-5}} \right) \quad (1)$$

where ΔP is excess pressure at a defined distance of 100 m from the vent (Johnson 2000). A 10-Pa signal recorded by the Shishaldin pressure transducer 6.5 km from the vent (an average value for the 19 April Strombolian activity) would have excess pressure of ~650 Pa at 100 m from the vent, and a corresponding *SPL* of 150 dB. The largest Shishaldin signals on 23 April, with $\Delta P=65$ Pa, correspond to an *SPL* of 166 dB. Johnson (2000) cites *SPL* levels at 100 m for a range of volcanoes including Erebus (*SPL*=145 dB), Karymsky (*SPL*=132 dB), and Sakurajima (*SPL*=136 dB). The only example of a volcano with *SPL* comparable to Shishaldin is the 1976 eruption of Tolbachik (Firstov and Kravchenko 1996), with

$SPL=160$ dB. Thus, even without detailed quantification of gas flux, we can be certain that bubble bursts at Shishaldin occurred at significantly higher pressures than those at other volcanoes.

The second distinction between Shishaldin explosions and those observed elsewhere is the spectral content. Bubble bursts at Shishaldin have spectral peaks between 0.7 and 1.5 Hz (Table 1). By contrast, spectral peaks are at 4–7 Hz at Stromboli (Vergnolle and Brandeis 1994), 3 Hz at Erebus (Rowe et al. 1998), and 2.5 Hz at Karymsky (Johnson et al. 1998). This suggests that gas bubbles at Shishaldin are significantly larger than those at these other volcanoes, with radii estimated at 5 m and lengths >10 m (Caplan-Auerbach et al. 2002). Although the exact conduit geometry is not known at Shishaldin, photographs taken on an overflight of the summit crater in 2000 show that the uppermost portion of the conduit is at least 25 m in diameter (P. Stelling, photograph and personal communication 2001). We assume that the conduit flares near the summit, but still has a radius of at least 5 m at depth. Even larger bubbles (~ 10 m radius) have been occasionally observed at Erebus (Johnson 2000), so we feel confident that a 5-m radius is reasonable for bubbles at Shishaldin.

Finally, we compare the occurrence frequency of Shishaldin explosions to other events in the literature. Shishaldin bubble bursts occur 3–20 times per minute with an average of 6–7 events per minute (Table 1). More frequent small signals may be lost in noise. Signal amplitudes and recurrence intervals do not appear to correlate. Some signals overlap in time series, suggesting that two gas bubbles occupied the conduit simultaneously, or that some bubbles underwent more than one oscillation prior to bursting. In comparison, acoustic signals recorded at Erebus occur several times per day, with occasional swarms of several per hour (Rowe et al. 1998). Similar bubble bursts at Stromboli and Etna have been recorded at intervals of 1–2 s (Ripepe et al. 1996, 2001), although several per hour are typical for Stromboli. Thus, Shishaldin gas bubbles are larger, oscillate with larger amplitude, and occur more frequently than bubbles at these other volcanoes. They are therefore more energetic and likely have higher gas flux. Although bubble bursts at Stromboli and Etna may occur more often than at Shishaldin, the gas bubbles are smaller and have lower amplitude. Erebus bubbles are comparable in size but occur less often.

In summary, an evaluation of Shishaldin acoustic activity suggests that this volcano has a wide conduit and is capable of producing large, energetic gas bubbles. We believe that the large amount of gas and acoustic energy released in the 1999 eruption explains the strong seismic tremor recorded at that time. In many eruptions, tremor amplitude has been found to correlate with VEI and ash column height (McNutt 1994). The Shishaldin eruption of 23 April, however, was associated with very strong tremor ($D_r=43$ cm²) but only a small, ash-poor plume. The strength of the signal recorded on the pressure sensor suggests that for Strombolian eruptions, reduced displace-

ment may be a better indicator of gas flux than ash column height. A more complete understanding of infrasonic signals is necessary before any of these signals may be used in a predictive capacity, but the data hint at a new means by which the state of the magmatic system and ensuing eruptive behavior may be evaluated in near-real time.

Conclusions

In spite of the fact that few visual observations were made of the 1999 eruption of Shishaldin, a great deal of information has been interpreted from seismic, satellite and acoustic data. This combination of instruments enabled us to monitor the transition from Strombolian to Subplinian, then back to Strombolian eruptive phases. In particular, the pressure sensor allowed us to investigate the specific timing and nature of these transitions. A 10-h period of 2–3 Hz acoustic humming at Shishaldin preceded the Subplinian phase, and may represent the release of a volume of gas from rising magma preceding the explosive Subplinian phase. Following the 49-min Subplinian eruption, which produced a broadband acoustic signal, the volcano returned to what appears to be a more common eruptive mechanism for Shishaldin – a Strombolian phase with massive gas bubble bursts. Four episodes of Strombolian activity ensued on 19–20 April, one of which was not associated with strong tremor and thus was not previously recognized. An additional period of explosivity occurred on 23 April, with explosions which were significantly larger and more frequent than similar events observed at other volcanoes. We suggest that the strongly reduced displacement of volcanic tremor recorded on 23 April may have been an indicator of high gas flux, rather than ash column height. Shishaldin exhibited an unusually wide range of eruptive behavior over a period of 4 days. Future efforts will seek to model the different phases of activity in greater detail.

Acknowledgments The authors would like to extend their gratitude to M. Garces who had the insight to deploy a pressure sensor on Shishaldin, and without whom this intriguing dataset would not exist. We are grateful to S. Vergnolle, A. Woods and an anonymous reviewer for thorough and insightful reviews of this manuscript. The manuscript also benefited from discussions with A. Harris, B. Houghton and many of our colleagues at the Alaska Volcano Observatory, notably C. Nye, P. Stelling, and G. Tytgat. This manuscript is submitted for publication with the understanding that the United States Government is authorized to reproduce and distribute reprints for governmental use. This work was supported by the USGS Volcano Hazards Program, under assistance award no. 98-HQ-AG-2122. The views and conclusions contained in this document are those of the authors and should not be interpreted as necessarily representing the official policies, either expressed or implied, of the US Government.

References

- Benoit JP, Thompson G, Lindquist K, Hansen R, McNutt SR (1998) Near-real-time WWW-based monitoring of Alaskan volcanoes: The IceWeb system. *EOS Trans Am Geophys Union* 79:F957
- Caplan-Auerbach J, McNutt SR, Vergnolle S, Boichu M (2002) Acoustic recordings of Strombolian and Subplinian activity at Shishaldin volcano, Alaska. *EOS Trans Am Geophys Union* 83:S386
- Coltelli M, Del Carlo P, Vezzoli L (1995) Stratigraphy of the Holocene Mt. Etna explosion eruptions. *Per Mineral* 64:141–143
- Dehn J, Dean KG, Engle K, Izbekov P (2002) Thermal precursors in satellite imagery of the 1999 eruption of Shishaldin volcano. *Bull Volcanol* (in press) DOI 10.1007/s00445-002-0227-0
- Dewey JM (1985) The propagation of sound from the eruption of Mt. St. Helens on May 18 1980. *Northwest Sci* 59:79–92
- Fairfield C (1980) OMSI Sound Project: the acoustic effects of the Mount St. Helens eruption on May 18, 1980. *Oregon Geol* 42:200–202
- Firstov PP, Kravchenko NM (1996) Estimate of the amount of explosive gas released in volcanic eruptions using air waves. *Volcanol Seismol* 17:547–560
- Garces M, Iguchi M, Ishihara K, Morrissey M., Sudo Y, Tsutsui T (1999) Infrasonic precursors to a Vulcanian eruption at Sakurajima Volcano, Japan. *Geophys Res Lett* 26:2537–2540
- Hagerty MT, Schwartz SY, Garces MA, Protti M (2000) Analysis of seismic and acoustic observations at Arenal Volcano, Costa Rica, 1995–1997. *J Volcanol Geotherm Res* 101:27–65
- Houghton BF, Sable JE, Wilson CJN, Coltelli M, Del Carlo P (2001) The influence of conduit processes during basaltic Plinian eruptions. *Trans AGU* 82(47):F1412
- Johnson JB (2000) Interpretation of infrasound generated by erupting volcanoes and seismo-acoustic energy partitioning, PhD Thesis, University of Washington
- Johnson JB, Lees JM (2000) Plugs and chugsseismic and acoustic observations of degassing explosions at Karymsky, Russia and Sangay, Ecuador. *J Volcanol Geotherm Res* 101:67–82
- Johnson JB, Malone SD (1997) Acoustic air-wave propagation from the 1980 Mount St. Helens Eruption. *EOS Trans AGU* 78(46):F130
- Johnson JB, Lees JM, Gordeev EI (1998) Degassing explosions at Karymsky Volcano, Kamchatka. *Geophys Res Lett* 25:3999–4002
- Lighthill J (1978) *Waves in fluids*. Cambridge University Press
- McNutt SR (1994) Volcanic tremor amplitude correlated with Volcanic Explosivity Index and its potential use in determining ash hazards to aviation. *Acta Vulcanologica* 5:193–196
- Miller TP, McGimsey RG, Richter DH, Riehle JR, Nye CJ, Yount ME, Dumoulin JA (1998) Catalog of the historically active volcanoes of Alaska. *US Geol Surv Open-File Rep* 98-482
- Moran SC, Stihler SD, Power JA (2002) A tectonic earthquake sequence preceding the April-May 1999 eruption of Shishaldin Volcano, Alaska. *Bull Volcanol* (in press) DOI 10.1007/s00445-002-0226-1
- Morrissey MM, Chouet BA (1997) Burst conditions of explosive volcanic eruptions recorded on microbarographs. *Science* 275:1290–1293
- Nye CJ, Keith TEC, Eichelberger JC, Miller TP, McNutt SR, Moran SC, Schneider DJ, Dehn J (2002) The 1999 eruptions of Shishaldin Volcano Alaska: an example of remote volcano monitoring. *Bull Volcanol* (in press) DOI 10.1007/s00445-002-0225-2
- Ripepe M, Poggi P, Braun T, Gordeev E (1996) Infrasonic waves and volcanic tremor at Stromboli. *Geophys Res Lett* 23:181–184
- Ripepe M, Coltelli M, Privitera E, Gresta S, Moretti M, Piccinini D (2001) Seismic and infrasonic evidences for an impulsive source of the shallow volcanic tremor at Mt. Etna, Italy. *Geophys Res Lett* 28:1071–1074
- Rowe CA, Aster RC, Kyle PR, Schlue JW (1998) Broadband recording of Strombolian explosions and associated very-long-period seismic signals on Mount Erebus volcano, Ross Island, Antarctica. *Geophys Res Lett* 25:2297–2300
- Sable J, Houghton B, del Carlo P, Coltelli M (2001) Mechanisms for basaltic Plinian volcanism: a quantitative study of the products of the 122 BC eruption of Mount Etna. *EOS Trans AGU* 82(47):F1369
- Schneider, DJ, Moran, SC, Nye CJ (1999) Volcanic clouds from the 1999 eruption of Shishaldin Volcano, Alaska: comparisons of satellite, seismic, and geologic observations. *EOS Trans AGU* 80(46):1146
- Stelling P, Beget J, Nye C, Gardner J, Devine JD, George RMM (2002) Geology and petrology of ejecta from the 1999 eruptions of Shishaldin Volcano, Alaska. *Bull Volcanol* (in press) DOI 10.1007/s00445-002-0229-y
- Thompson G, McNutt SR, Tytgat G (2002) Three distinct regimes of volcanic tremor associated with eruptions of Shishaldin Volcano, Alaska, April 1999. *Bull Volcanol* (in press) DOI 10.1007/s00445-002-0228-z
- Vergnolle S, Brandeis G (1994) Origin of the sound generated by Strombolian explosions. *Geophys Res Lett* 21:1959–1962
- Vergnolle S, Brandeis G (1996) Strombolian explosions 1. A large bubble breaking at the surface of a lava column as a source of sound. *J Geophys Res* 101:20433–20447
- Walker GPL, Self S, Wilson L (1984) Tarawera 1886, New Zealand; a basaltic plinian fissure eruption. *J Volcanol Geotherm Res* 21:61–78
- Williams SN (1983) Plinian airfall deposits of basaltic composition. *Geology* 11:211–214